1.7 kW 6.78 MHz Wireless Power Transfer with Air-Core Coils at 95.7% DC-DC Efficiency

Lei Gu, Juan Rivas-Davila
Department of Electrical Engineering, Stanford University, USA
leigu@stanford.edu, jmrivas@stanford.edu

***Abstract*—This paper describes the design and implementation of a 1.7 kW wireless power transfer system that operates at 6.78 MHz and uses low-cost air-core coils. The demonstration achieves a dc-dc efficiency of 95.7% at 1.7 kW and maintains above 93% efficiency between 100 W and 1.7 kW.**

***Index Terms*—Inductive power transmission, power amplifiers.**

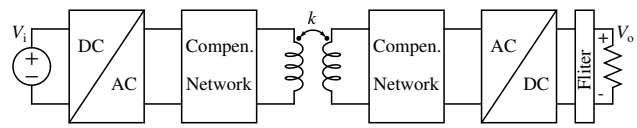

Fig. 1: A typical inductive WPT system.

I. Introduction

The wireless power transfer (WPT) technology can benefit many battery-powered systems, such as electric vehicles, autonomous robots, and implantable medical devices. A typical inductive WPT system consists of an inverter, a pair of electromagnetic coils, and a rectifier, as shown in Fig. 1. The inverter drives the transmitting coil to generate a high-frequency electromagnetic field, which couples to the receiving coil and transmits power wirelessly. The majority of the commercial WPT systems operate with a frequency f_s of $20\,\mathrm{kHz}$-$200\,\mathrm{kHz}$ [1], which causes magnetic coils to dominate the losses, size, and cost of the wireless charging system [2].

Increasing the frequency of operation has the potential to improve coil's efficiency and power density as a coil's quality factor naturally increases with frequency in certain range [3]. Beyond $200\,\mathrm{kHz}$, the international, scientific, and medical (ISM) band, e.g., $6.78\,\mathrm{MHz}$, is an attractive frequency of operation from a regulatory and standardization perspective [4].

Increasing the WPT frequency to multi-MHz range can also significantly reduce the coil's cost. At MHz frequencies, the benefit of using Litz wires is limited and high-Q coils can be made even using low-cost solid magnet wires [3]. However, despite the potential benefit of cost reduction, increasing the f_s beyond $6.78\,\mathrm{MHz}$ brings significant challenges to the WPT system design, particularly achieving a competitive efficiency performance. Table I compares the performance of state-of-the-art (SOA) inductive WPT systems. Most systems with an f_s above $6\,\mathrm{MHz}$ only achieved efficiencies in the up 80s%, possessing more than $2\times$ higher losses than the highly-efficient performance in the $20\,\mathrm{kHz}$-$200\,\mathrm{kHz}$ frequency range (95%) [5], [6]. The challenges mainly come from achieving high efficiencies in the multi-MHz inverter and high kQ product in air-core coils.

With a high-Q self-resonant coil [7], Gu *et al.* [8] for the first time demonstrated $6.78\,\mathrm{MHz}$ WPT systems that achieved a dc-dc efficiency of 95% at $1\,\mathrm{kW}$. The novel coil structure in [7] utilizes magnetic ferrite and capacitance ballasting to force equal current sharing among multiple winding layers, mitigating both the skin and proximity effects that typically drive winding losses at multi-MHz frequencies. This self-resonant coil using ferrite achieves a Q that is $4\times$ higher than the best conventional designs (with similar dimensions) at $6.78\,\mathrm{MHz}$.

In contrast to the work in [8], this paper focuses on the design and optimization of a high-power multi-MHz inductive WPT system using low-cost air-core coils. We present in this paper a 6.78 MHz, 200 V to 410 V inductive WPT system that achieves 95.7% dc-dc efficiency at 1.7 kW, a significant improvement in efficiency and power level compared to previous MHz WPT systems as shown in Table I.

The rest of the paper is organized as follows. Section II discusses the design of different stages of the multi-MHz WPT system. Section III describes the detailed implementation and experimental results of the prototype demonstration. Section IV summarizes the paper.

II. System Design

To achieve a high dc-dc efficiency, each of three stages in Fig. 1, inverter, coils, and rectifier, needs to operate efficiently. The following section will discuss the design and optimization of each stage in the reverse order.

A. Rectifier

Full-bridge diode rectifier is the most commonly used rectifier circuit. Depending on the output filter, we can have either voltage-mode or current-mode rectifier. A series-compensated receiving coil needs a voltage-mode rectifier, while a parallel-compensated receiving coil needs a current-mode rectifier.

Because of the parasitic capacitance of diodes, the rectifier's input impedance is capactive at the fundamental frequency. The capacitive reactance depends on the large-signal behavior of the rectifier and does not simply equal the sum of the small-signal junction capacitance of the diodes. At kHz frequencies,

978-1-7281-9633-6/21/$31.00 ©2021 IEEE

TABLE I: PERFORMANCE COMPARISON OF THE STATE-OF-THE-ART WIRELESS POWER TRANSFER SYSTEMS

Reference	[9]	[5]	[6]	[10]	[11]	[12]	[13]	[8]	This work
f_s [MHz]	0.085	0.1	0.8	6.78	6.78	6.78	13.56	6.78	6.78
Power [W]	3.3k-11k	5k	30	20	10	50	300	1k	1.7k
Peak dc-dc η [%]	90−93	96.5	95.7	84	85	88	90	95.1	95.7
Coil Design	N/A	Litz & Ferrite	Litz & Air-core	PCB & Air-core	PCB & Air-core	Solid & Air-core	Solid & Air-core	PCB & Ferrite	Solid & Air-core
Coil Coupling	N/A	0.33	0.27	0.13	0.11	0.11	0.26	0.15	0.28
Semiconductor Tech.	N/A	SiC & Si	All GaN	Si & SiC	GaN & Si	GaN & Si	GaN & Si	Si & SiC	GaN & SiC

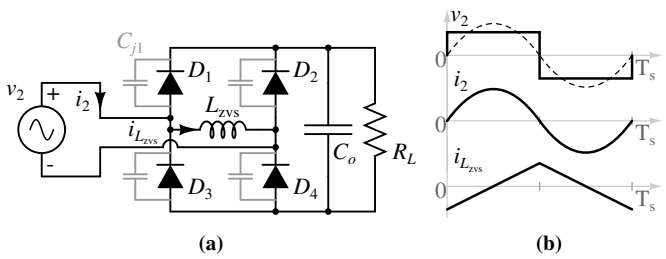

Fig. 2: A voltage-mode rectifier with a parallel tuning inductor. **(a)** Circuit. **(b)** Ideal waveform.

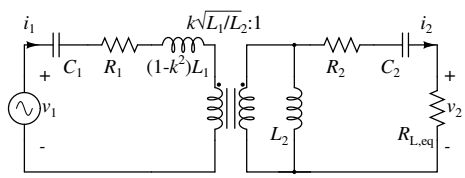

Fig. 3: WPT with SS compensation, the inverter is modeled as a voltage source, while the rectifier is modelled as a resistive load $R_{\text{L,eq}}$. $L_{1,2}$ are self-inductances of the coils, $C_{1,2}$ are series compensation capacitances, k is coupling coefficient of the coils, and $R_{1,2}$ are total series resistances of the coils and capacitors.

this capacitive reactance has negligible effect on the inverter and coils' operation. At multi-MHz frequencies, this capacitive reactance can affect the inverter's efficiency and the coils' voltage conversion ratio. Connecting an inductor in parallel to the rectifier's input can help tune the total impedance to be resistive, as shown in Fig. 2.

B. Wireless Coils

The wireless link, or the coupled coils at the center of the WPT system, can be modelled as a transformer. Due to the low coupling coefficient, the coils need proper resonant compensation to cancel the large leakage inductance and transfer power efficiently. There are four basic compensation topologies, including series-series (SS), series-parallel (SP), parallel-series (PS), and parallel-parallel (PP).

To achieve the optimal efficiency for the wireless link, the inductance and capacitance have to be properly sized with regard to the ac load resistance (the rectifier's large-signal impedance) and the voltage conversion ratio. Ref. [5] derived the optimal designs for SS and SP compensations. Ref. [8] presented the solutions for PP compensation. In this demonstration, we used the SS compensation for the wireless link and the following is a short review of optimal SS compensation.

TABLE II: PARAMETERS DESCRIBING THE RESONANT CIRCUIT

Definition	Equation
Angular Frequency	$\omega_{\text{S}} = 2\pi f_{\text{S}}$
Load Matching Factor	$\gamma = R_{\text{L,eq}}/(\omega_{\text{S}} L_2)$
Capacitive Impedance Factor	$\chi_i = 1/(\omega_{\text{S}}^2 L_i C_i)$
Coil Quality Factor	$Q_i = \omega_{\text{S}} L_i / R_i$
Inductor Quality Factor	$Q = \sqrt{Q_1 Q_2}$

Fig. 3 shows the equivalent circuit for a WPT system using SS compensation. Table II defines the parameters that describe the resonant circuit. For the capacitance needed in an optimal SS compensation,

$$\chi_1 = 1,\ \chi_2 = 1, \tag{1}$$

where the capacitance is selected to cancel the self-inductance on each side. Practically, it can be quickly tuned by ensuring that L and C resonate at the switching frequency with the opposite coil terminals open.

Further, the maximum WPT link efficiency is achieved when the load matching factor, the ratio of the load to the receiving coil's impedance, is

$$\gamma_{\text{opt}} = \frac{1}{Q_2}\sqrt{1 + k^2 Q_1 Q_2}. \tag{2}$$

With high-Q symmetric coils, $kQ_1 >> 1$, $kQ_2 >> 1$, $Q_1 \approx Q_2$,

$$\gamma_{\text{opt}} \approx k. \tag{3}$$

With (1) and (2), as derived in [5], [14], the maximum wireless link efficiency is

$$\eta_{\text{max}} = \frac{k^2 Q^2}{\left(1 + \sqrt{1 + k^2 Q^2}\right)^2}. \tag{4}$$

With optimal compensation capacitance in (1), the voltage conversion ratio becomes

$$|G_v| = \left|\frac{v_2}{v_1}\right| = \frac{\gamma}{k}\sqrt{\frac{L_2}{L_1}}. \tag{5}$$

If $\gamma = \gamma_{\text{opt}}$, $|G_v|_{\text{opt}} \approx \sqrt{L_2/L_1}$.

C. Inverter

The high-frequency inverter ideally can use any of the switching amplifiers with a theoretical efficiency of 100%,

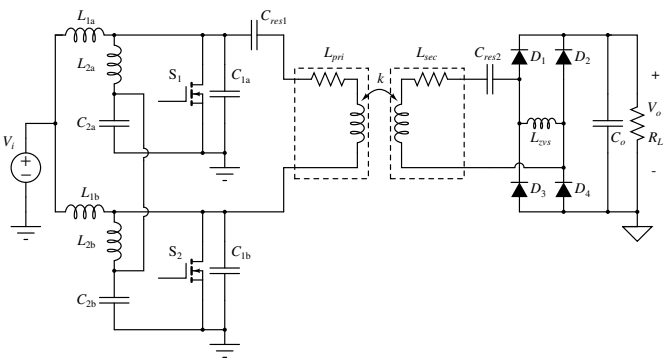

Fig. 4: Schematic of the PPT Φ_2 wireless dc-dc converter.

such as Class-D, Class-E, Class-F, and Class-EF [5], [8], [11], [15]. For low-frequency ($\leq$ 1 MHz) inductive WPT systems, Class-D is the most common choice, often implemented with a half-bridge or full-bridge circuit [5], [6]. Class-D amplifier has the highest transistor utilization factor among different switching amplifiers [16]. Here, the transistor utilization factor is defined as the output power normalized to the product of switch voltage stress and rms current.

As the frequency further increases and approaches 6.78 MHz, it becomes more challenging to implement a high-side gate driver that can withstand a large dV/dt at the switching node. Besides the complexity of high-side gate driving, to achieve zero-voltage switching (ZVS) in a high-frequency Class-D amplifier, the switches' output capactiance C_{oss} become non-negligible and may require a significant dead-time for resonant charging/discharging, which compromises the practical transistor utilization factor. With non-negligible C_{oss}, the switches can operate with both ZVS and zero voltage derivative switching (ZVDS) so that the circuit behaves more like a hybrid Class-DE amplifier [17].

Contrary to low-frequency inductive WPT systems where Class-D inverter dominates, many multi-MHz WPT systems prefer the Class EF family switching amplifiers due to the simplicity of gate driving [8], [12], [13], [15]. However, unlike Class-D, the efficiency optimization of Class-E, -EF amplifiers for WPT is often more complex, as it involves multiple degrees of freedom in resonant component selection. Regardless of which topology to use, it is critical to maintain efficient ZVS operation across a wide range of loads in an inverter operating at MHz frequencies.

In this demonstration, we use a novel push-pull EF_2/Φ_2 amplifier topology that utilizes a T network for impedance tuning, which is termed a PPT Φ_2 amplifier and introduced in [18]. The PPT Φ_2 amplifier has the advantages of high transistor utilization factor, simplicity of gate driving, and capability of resistive load independent ZVS operation. Fig. 4 shows the schematic of the PPT Φ_2 amplifier driving the series-compensated coils and a full-bridge rectifier.

TABLE III: BILL OF MATERIALS, PPT Φ_2 WPT DC-DC CONVERTER

Devices	Component Description
(a) Inverter	
$S_{1,2}$	GaN Systems GS66508B, 650 V GaN FET
Gate driver	Texas Instruments LMG1025
L_{1a}, L_{1b}	4.33 µH, Ferroxcube E22/6/16-4F1 x 2
L_{2a}, L_{2b}	1.085 µH, Fair-rite 67 EEQ25/16
C_{2a}, C_{2b}	127 pF, C0G, 3 kV
C_{1a}, C_{1b}	$S_{1a,1b}$ C_{oss} + STPSC406B C_j + 136 pF , C0G, 1 kV
(b) Rectifier	
$D_{1\text{-}4}$	STMicro STPSC406B-TR x 2, 650 V SiC Schottky
L_{zvs}	3.7 µH, Fair-rite 67 EEQ25/16
(c) Coils	
L_{pri}, L_{sec}	6.25 µH, AWG 10, 6 turns, $Q \approx 700$
C_{res1}, C_{res2}	88 pF, C0G, 3kV

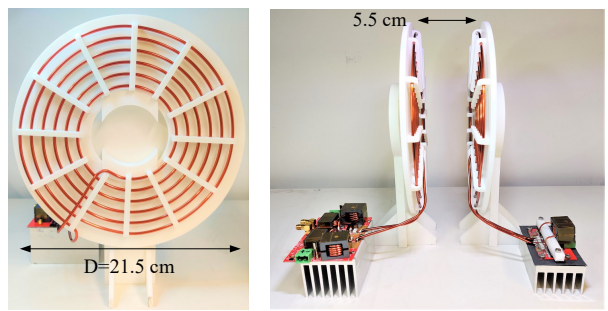

(a) **(b)**

Fig. 5: Photograph of the 1.7 kW prototype coils, $k \approx 0.28$ at 5.5 cm gap.

III. SYSTEM IMPLEMENTATION

Table III lists the key components for the 1.7 kW Φ_2 wireless dc-dc converter. With a targeted output of 400 V and 1650 kW, the dc load resistance is $R_{\mathrm{L}} = 400^2/1650\ \Omega = 97\ \Omega$. For convenience, we used 100 Ω in testing. The equivalent ac load for the receiving coil is $R_{\mathrm{L,eq}} = \frac{8}{\pi^2} R_{\mathrm{L}} = 81\ \Omega$. With manufacturer's SPICE model of the SiC didoe, we found through simulation that a 3.7 µH L_{zvs} makes the rectifier's impedance net resistive.

With an estimated k of 0.3 between the coils, the optimal inductance of the receiving coil, according to (3), should be

$$L_{sec} = \frac{R_{\mathrm{L,eq}}}{\gamma_{\mathrm{opt}}\omega_s} \approx \frac{R_{\mathrm{L,eq}}}{k\omega_s} = 6.34\ \mu\mathrm{H} \tag{6}$$

The PPT Φ_2 can generate a square wave with an amplitude of roughly $2V_i$, so the transmitting coil should have the same inductance as the receiving coil with a targeted input of 200 V. The component values of the PPT Φ_2 amplifier were designed following the guidelines in [18]. Fig. 5 presents the prototype wireless coils, and Fig. 6 shows the prototype inverter and rectifier. The final coils have a inductance around 6.25 µH.

Fig. 7 shows the measured drain node voltage waveform and efficiency performance of the prototype. The converter can deliver 1700 W continuously from 200 V to 410 V with a dc-dc efficiency of 95.7 % at 6.78 MHz, and can maintain above 93% dc-dc efficiency across 100 W to 1700 W output range. Fig. 8 shows the test setup of the prototype with forced-air cooling and thermal camera.

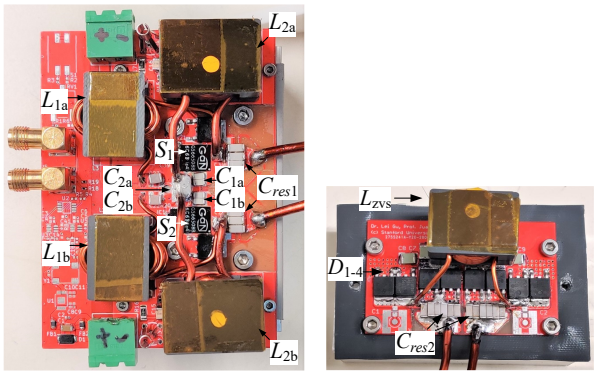

(a) **(b)**

Fig. 6: Photograph of the PPT Φ_2 wireless dc-dc converter. **(a)** PPT Φ_2 inverter, dimensions (including heatsink) are 8.1 cm x 7 cm x 6 cm. **(b)** Rectifier, dimensions (including heatsink) are 4.6 cm x 3.6 cm x 3.6 cm.

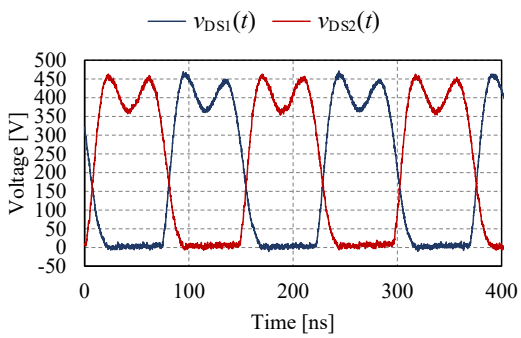

(a)

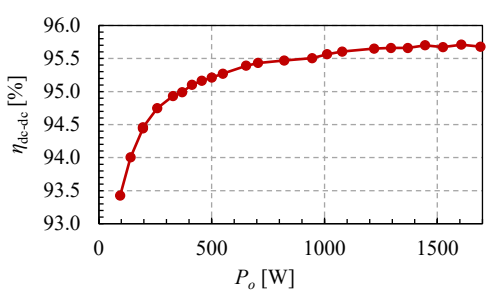

(b)

Fig. 7: Prototype experimental results, **(a)** drain voltage waveform at 200 V_i and **(b)** efficiency performance across output power. Gate driving losses excluded. Power is varied by adjusting the input voltage.

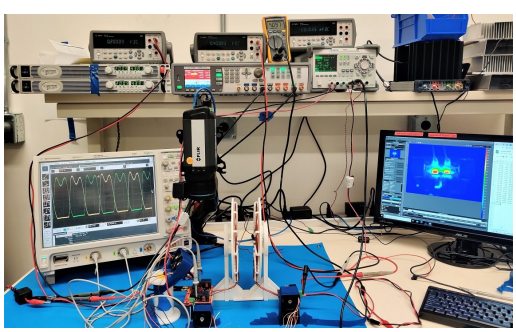

Fig. 8: Test setup with fan cooling and thermal camera.

IV. Conclusion

High-frequency wireless power transfer can be more cost-effective than conventional litz-based, kHz-frequency WPT systems, but the efficiency of existing MHz-frequency systems has been limited by low-efficiency multi-MHz inverters. The losses in MHz demonstrations have been about 2× higher than comparable systems in the kHz regime. In this paper, we introduce a novel high-frequency resonant amplifier topology to showcase a 1.7 kW 6.78 MHz WPT system with dc-dc efficiencies above 95 % while using low-cost air-core coils. This benchmark-setting prototype highlights the promise of high-frequency, high-power WPT for future ubiquitous EV charging applications.

References

[1] "Wireless Power Transfer for Light-Duty Plug-In/Electric Vehicles and Alignment Methodology," USA, November 2017.

[2] A. Shekhar, V. Prasanth, P. Bauer, and M. Bolech, "Economic viability study of an on-road wireless charging system with a generic driving range estimation method," *Energies*, vol. 9, no. 2, p. 76, 2016.

[3] C. R. Sullivan *et al.*, "On size and magnetics: Why small efficient power inductors are rare," in *2016 International Symposium on 3D Power Electronics Integration and Manufacturing (3D-PEIM)*. IEEE, 2016, pp. 1–23.

[4] Intl. Commission on Non-Ionizing Radiation Protection and others, "Guidelines for limiting exposure to Electromagnetic Fields (100 kHz to 300 GHz)," *Health Physics*, vol. 118, no. 5, pp. 483–524, 2020.

[5] R. Bosshard *et al.*, "Modeling and η-α-Pareto Optimization of Inductive Power Transfer Coils for Electric Vehicles," *IEEE Journal of Emerging and Selected Topics in Power Electronics*, vol. 3, no. 1, pp. 50–64, 2014.

[6] O. Knecht *et al.*, "High-Efficiency Transcutaneous Energy Transfer for Implantable Mechanical Heart Support Systems," *IEEE Transactions on Power Electronics*, vol. 30, no. 11, pp. 6221–6236, 2015.

[7] A. L. Stein *et al.*, "Wireless Power Transfer Utilizing a High-Q Self-Resonant Structure," *IEEE Transactions on Power Electronics*, vol. 34, no. 7, pp. 6722–6735, 2018.

[8] L. Gu *et al.*, "6.78-MHz Wireless Power Transfer With Self-Resonant Coils at 95% DC–DC Efficiency," *IEEE Transactions on Power Electronics*, vol. 36, no. 3, pp. 2456–2460, 2021.

[9] WiTricity. [Online]. Available: https://witricity.com/

[10] M. Liu *et al.*, "Parameter Design for a 6.78-MHz Wireless Power Transfer System Based on Analytical Derivation of Class E Current-Driven Rectifier," *IEEE Trans. Power Elec.*, vol. 31, no. 6, pp. 4280–4291, 2016.

[11] J. Li and D. Costinett, "Comprehensive Design for 6.78 MHz Wireless Power Transfer Systems," in *2018 IEEE Energy Conversion Congress and Exposition (ECCE)*, 2018, pp. 906–913.

[12] J. M. Arteaga *et al.*, "Multi-MHz IPT Systems for Variable Coupling," *IEEE Trans. Power Elec.*, vol. 33, pp. 7744–7758, 2018.

[13] K. Surakitbovorn and J. Rivas, "Design of a GaN-based Wireless Power Transfer System at 13.56 MHz to Replace Conventional Wired Connection in a Vehicle," in *2018 International Power Electronics Conference (IPEC-Niigata 2018-ECCE Asia)*, 2018, pp. 3848–3854.

[14] E. Waffenschmidt and T. Staring, "Limitation of Inductive Power Transfer for Consumer Applications," in *IEEE European Conference on Power Electronics and Applications*, 2009, pp. 1–10.

[15] X. Zan and A.-T. Avestruz, "27.12 MHz Bi-Directional Wireless Power Transfer Using Current-Mode Class D Converters with Phase-Shift Power Modulation," in *2018 IEEE PELS Workshop on Emerging Technologies: Wireless Power Transfer (Wow)*. IEEE, 2018, pp. 1–6.

[16] Z. Kaczmarczyk, "High-Efficiency Class E, EF_2, and E/F_3 Inverters," *IEEE Transactions on Industrial Electronics*, vol. 53, no. 5, pp. 1584–1593, 2006.

[17] D. C. Hamill, "Class DE inverters and rectifiers for DC-DC conversion," in *PESC Record. 27th Annual IEEE Power Electronics Specialists Conference*, vol. 1. IEEE, 1996, pp. 854–860.

[18] L. Gu *et al.*, "Push-Pull Class Φ_2 RF Power Amplifier," *IEEE Transactions on Power Electronics*, 2020.